Available online at www.sciencedirect.com
SCIENCE DIRECT
Estuarine, Coastal and Shelf Science 64 (2005) 156–170
ESTUARINE COASTAL AND SHELF SCIENCE
www.elsevier.com/locate/ECSS

Temporal variability of optical properties in a shallow, eutrophic estuary: Seasonal and interannual variability

C.L. Gallegos*, T.E. Jordan, A.H. Hines, D.E. Weller

Smithsonian Environmental Research Center, P.O. Box 28, Edgewater, MD 21037, USA

Received 20 September 2004; accepted 28 January 2005
Available online 2 April 2005

Abstract

We monitored inherent optical properties in a turbid, eutrophic estuary to determine the factors affecting the temporal variability in water clarity. Time series of absorption and scattering coefficients were measured at 1-h intervals for nearly 2 years. The seasonal pattern in weekly averaged absorption and scattering coefficients in each year was driven primarily by changes in the particulate matter of both biogenic and mineral origin. Temporal patterns in particulate absorption and scattering resulted from identifiable events that differed in relative magnitude between the 2 years: a spring bloom was followed by a transient "clear-water" phase, followed by increases in non-algal particulate matter to a late-summer maximum, and rapid declines of all parameters in late fall. Interannual variability in the spring bloom was governed by timing and magnitude of nutrient inputs from the watershed, while major patterns in summer variability of both organic and inorganic particulate matter appeared to follow the general cycle of biological activity in the system.

Keywords: optical properties; estuary; absorption coefficient; scattering coefficient; suspended solids

1. Introduction

The penetration of light underwater is of fundamental importance to aquatic ecosystems. The quantity and quality of underwater light drive photosynthesis by phytoplankton, benthic algae, and submersed macrophytes (Kirk, 1994). Light is required for feeding by visually orienting predators (Aksnes et al., 2004), and the visual appearance of a water body is a key factor in the aesthetic and recreational appeal to humans (Davies-Colley et al., 1993). Understanding the factors controlling the variability of optical properties in coastal waters is important, because changes in the optical properties of a water body can be both indicators of stressors such as eutrophication, and can be potential stressors to components of the ecosystem, e.g. submerged aquatic vegetation (SAV), that require high light intensities for survival.

In coastal watersheds worldwide, human population growth has been increasing at a high rate and has negatively impacted living resources at many locations (Richardson and Jørgensen, 1996; Rabalais and Turner, 2001). Many of the processes that threaten estuarine habitat quality result in detectable changes to the optical properties of the water. For example, eutrophication results in increasing frequency and magnitude of phytoplankton blooms that absorb and scatter light in spectrally identifiable ways (Gallegos and Jordan, 2002). Highway construction and certain agricultural practices increase erosion and delivery of suspended sediments that increase the scattering and reflectivity of estuarine waters (Stumpf and Pennock 1989, 1991). Altered flow paths from wetlands and certain industrial discharges (e.g. paper mill effluents) increase the concentration of

* Corresponding author.
E-mail address: gallegosc@si.edu (C.L. Gallegos).

0272-7714/$ - see front matter © 2005 Elsevier Ltd. All rights reserved.
doi:10.1016/j.ecss.2005.01.013

colored dissolved organic matter (CDOM) of some estuaries, greatly increasing the absorption of blue and ultraviolet light (McPherson and Miller 1987; Gallegos and Kenworthy, 1996). Thus changes in the optical properties of estuarine waters are a potentially sensitive indicator of stressors characteristic of human disturbance. Long series of observation, however, are needed to discern human induced changes from normal seasonal and interannual variability.

Estuaries are optically complex systems due to the sources, sinks, and transformations of terrestrially derived dissolved and particulate matter that mixes with coastal-derived water that is likewise optically complex (Davies-Colley et al., 1993). Flocculation of river-borne clay particles occurs with small increases in salt concentration, changing the effective size distribution and settling rate of suspended solids (Postma, 1967). Interactions between particulate matter and biological production also occur on longer (i.e. seasonal) time scales, resulting in, e.g. co-flocculation of phytoplankton and inorganic mineral particles (Stross and Sokol, 1989). A variety of physical (Sanford, 1994) and biological (Hines et al., 1990) processes operate to resuspend bottom sediments on a variety of time scales. Such processes change not only the concentration of optically active particulate matter in the water column, but also alter the size-distributions of particulate matter, thereby affecting the absorption and scattering per unit mass of suspended solids (Mobley, 1994). Sorting out the relative timing and magnitude of such influences on estuarine optical properties is challenging due to the complexity of processes and difficulty in making the relevant measurements.

Advances in instrumentation have made it possible to monitor changes in inherent optical properties of water bodies (Dickey et al., 1998; Chang and Dickey, 2001), i.e. those properties that depend only on the amounts and kinds of material in the water. Absorption and scattering spectra are especially informative because from them it is possible to estimate concentrations of materials in the water responsible for absorption and attenuation (Chang and Dickey, 2001; Gallegos and Neale, 2002). For example, Chang and Dickey (1999) examined time series of absorption and scattering spectra from moored instrumentation off Georges Bank, and observed high concentrations of suspended solids in a near-bottom mooring following the passage of a hurricane. Gallegos and Jordan (2002) measured changes in absorption and scattering spectra during the course of a large bloom of the dinoflagellate *Prorocentrum minimum*. They observed a three-fold increase in attenuation due to the bloom and determined that the optical effects of the bloom were initially dominated by phytoplankton absorption, and then by non-algal detrital matter at the termination of the bloom.

Here we present the results of a nearly 2-year series of hourly measurements of inherent optical properties in the Rhode River. Our objectives were to determine the magnitude and variability of factors responsible for reduced water clarity in this system which once supported an abundance of submerged vegetation (Southwick and Pine, 1975). These observations are unique in their coverage of the seasonal and interannual variability, and in their resolution of the components of absorption. Key features of the variability are interannual differences in the magnitude of the spring bloom, and the relative constancy of the late summer peak of non-algal particulate matter. Additionally, we examine a variety of long-term ancillary data to propose causal mechanisms for the seasonal pattern of non-algal particulates.

2. Study site

Inherent optical properties were monitored at a site on the Rhode River (38.883°N, 76.533°W), Maryland. The Rhode River is a small, shallow tributary embayment, or subestuary, on the western shore of Chesapeake Bay (Fig. 1). The subestuary is located in the mesohaline zone of Chesapeake Bay, where the salinity varies seasonally from 5 to 18 at the mouth depending on flow of the Susquehanna River, and from 0 to 14 at the head, depending on flow of the Susquehanna River and local flow of Muddy Creek, the principal freshwater source to the Rhode River. Depth varies from about 4 m at the mouth to <1 m at an area of subtidal mud flats upestuary of the monitoring station. The subestuary is usually vertically homogenous, though subsurface chlorophyll accumulations sometimes occur during dense phytoplankton blooms (Gallegos et al., 1990).

The subestuary is eutrophic, with summer chlorophyll concentrations averaging 20–40 mg m^{-3}, and experiences extraordinary spring blooms of the dinoflagellate *Prorocentrum minimum* in years when the spring freshet of the Susquehanna River is sufficient to infuse nitrate into the system in mid- to late April (Gallegos et al., 1990, 1997; Gallegos and Jordan, 2002). Inputs of suspended solids from the local watershed peak in spring (Jordan et al., 1986), though concentrations of suspended solids in the water column peak in late summer (Jordan et al., 1991, and see below).

3. Materials and methods

3.1. Optical monitoring

Spectral absorption [$a(\lambda)$] and attenuation [$c(\lambda)$] coefficients were measured at 9 wavelengths: 412, 440, 488, 510, 532, 555, 650, 676, and 715 nm, using a flow-through absorption-attenuation meter (ac9, Wetlabs).

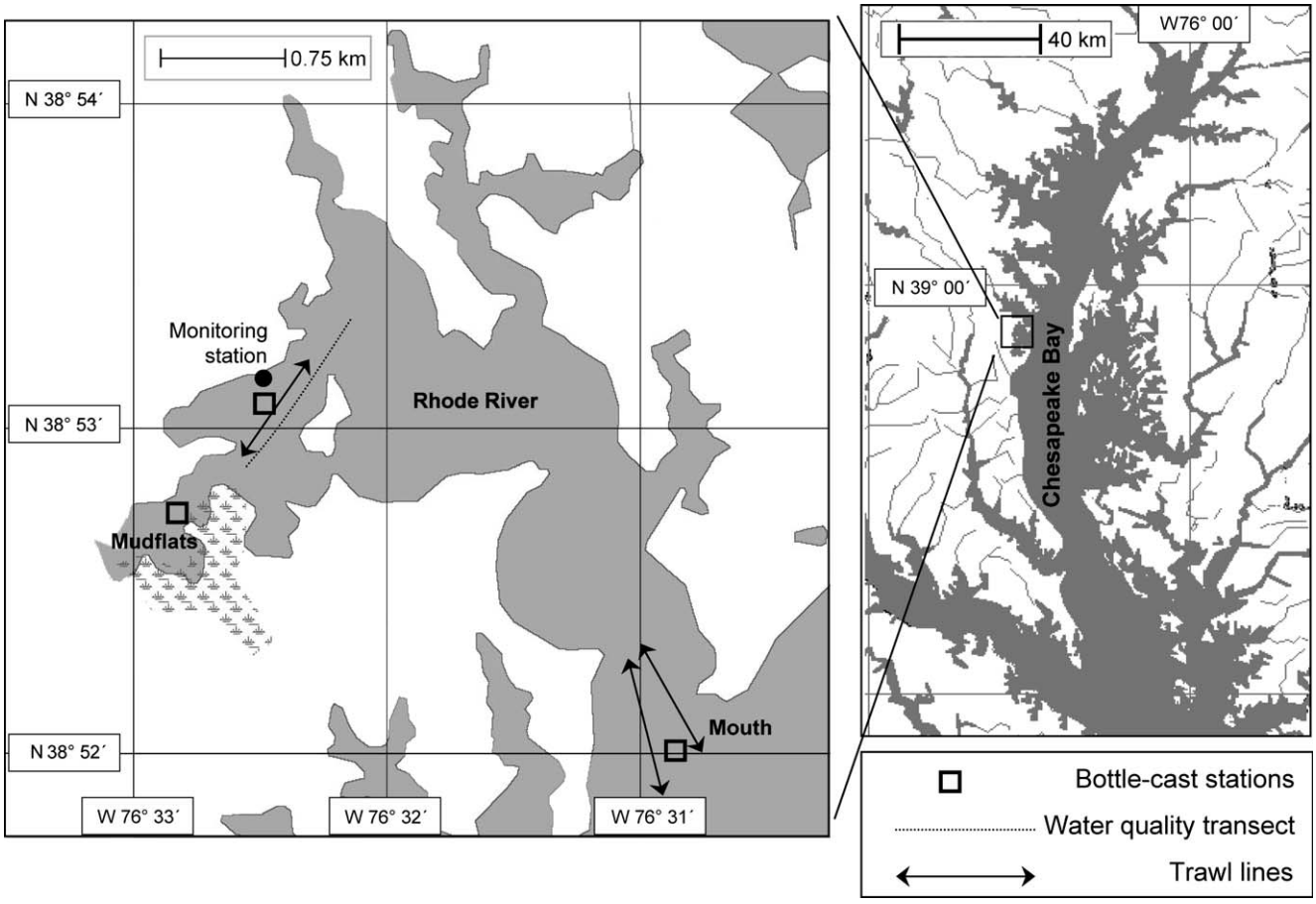

Fig. 1. Map of the Rhode River, Maryland, showing locations of optical monitoring station, bottle-cast stations, water quality transect, and trawl lines. Inset shows location of the Rhode River on the western shore of Chesapeake Bay.

Flow to the ac9 was by gravity feed. Water from the estuary was pumped into an open topped polyvinyl chloride (PVC) cylinder with an overflow pipe to provide a constant head. A spigot and tubing located near the bottom of the cylinder conducted water past a bubble trap standpipe to the ac9. A Wetlabs MPak was used to control the ac9 and log the data. Once per hour the ac9 was turned on, allowed to warm up for 5 min, and sampled for 1 min at 6 Hz.

The PVC cylinder, ac9, and MPak were housed in a monitoring shed at the end of the Smithsonian pier on the Rhode River (Fig. 1). To reduce fouling within the cylinder, the pump was operated only 15 min h^{-1}, extending from about 10 min before to 5 min after sampling by the ac9. At the conclusion of a sampling cycle, a solenoid valve was opened that allowed about 60 ml of bromide solution to flow through the standpipe and ac9 to inhibit growth of fouling organisms on the optical surfaces of the ac9. Timing of the pump and solenoid valve was controlled by a Campbell Scientific CR10 data logger and control module.

The system was not operated when the estuary was ice-covered, to avoid damage to the sampling pump. In January and February of 2000 when ice cover was prolonged, we augmented the series by collecting grab samples through a hole in the ice for 23 days. These samples were run through an ac9 in the laboratory as described by Gallegos and Neale (2002).

3.2. Data processing

Data were downloaded and the ac9 was cleaned 3 times per week. Cleaning was commenced immediately following a reading. Water from that reading was collected and run through the meter again after cleaning to correct for drift due to fouling or accumulation of particulate matter during the previous monitoring period. Cleaning and downloading generally took less than 1 h, so that hourly sampling was usually not interrupted.

We calculated the change in absorption [$a(\lambda)$] and beam attenuation [$c(\lambda)$] coefficients after cleaning and applied the difference incrementally over the time period since the last cleaning, which was generally <3 d. We calculated the increment linearly from late fall to early spring when drift was due to settling of inanimate particulate matter in the tubes, and exponentially during

spring and summer when drift was due primarily to biological fouling. Inappropriate application of a linear correction could be recognized by the calculation of negative coefficients near the beginning of the monitoring period. Temperature and salinity at the site were monitored at hourly intervals coinciding with ac9 measurements by a Hydrolab (™) Minisonde. These measurements were used to calculate corrections for the temperature and salinity dependence of the absorption coefficient of pure water according to the manufacturer's specifications. In these waters, the resulting corrections were always small in relation to the overall magnitude and relative variability in measured optical coefficients.

3.3. Data analysis

We estimated the components of absorption by a modification of the procedure of Gallegos and Neale (2002). Briefly, the absorption coefficient referenced to water, $a_{t-w}(\lambda)$, at wavelength λ may be represented as the sum of absorption due to colored dissolved organic matter (CDOM), phytoplankton pigments, and non-algal particulate matter,

$$a_{t-w}(\lambda) = a_g(\lambda) + a_\phi(\lambda) + a_{p-\phi}(\lambda) \quad (1)$$

where the subscripts refer to absorption by particular components: g for CDOM (i.e. *gelbstoff*, Kirk, 1994), ϕ for phytoplankton, and $p-\phi$ for non-algal particulate matter. The average spectral shape of absorption by a component was represented by a normalized absorption function, determined by dividing the absorption by a component at each wavelength by the value at a reference wavelength. The normalized absorption spectra were determined using laboratory measurements in which the components were physically separated, as reported previously (Gallegos and Neale, 2002). The estimation procedure determines the value of absorption by each component at the reference wavelength, from which absorption at all other wavelengths may be calculated by multiplication by the normalized absorption function. Reference wavelengths were chosen as 440 nm for CDOM and non-algal particulates by convention (Kirk, 1994), and 676 nm for phytoplankton because it is at an absorption peak of chlorophyll. Further details and the modifications to the procedure of Gallegos and Neale (2002) are given in Appendix A.

We represented the wavelength dependence of particulate scattering spectrum as the product of an exponential function of wavelength scaled by the particulate scattering at a reference wavelength (555 nm),

$$b_p(\lambda) = b_p(555)\left(\frac{555}{\lambda}\right)^{\eta} \quad (2)$$

where $b_p(\lambda)$ = the particulate scattering spectrum, and η is the scattering spectral exponent. We estimated η as the negative slope of a log–log regression of the 9 measured $b_p(\lambda)$ against λ. Eq. (2) well characterizes the spectrum when scattering is dominated by particles having sizes smaller or comparable to the wavelength of light, whereas when scattering is dominated by larger particles, estimated η is small and wavelength dependence of scattering is characterized by depressions associated with the red and blue absorption peaks of chlorophyll (Stramski and Mobley, 1997). Scattering by pure water and by CDOM are considered negligible (Kirk, 1994).

3.4. Laboratory measurements of optical properties

To develop the normalized absorption functions of the optically active components and to examine spatial gradients in optical properties, we collected vertically integrated whole-water samples from 3 stations: up-estuary of the optical monitoring station in a region of subtidal mudflats, near the monitor, and down estuary of the monitor at the mouth of the Rhode River (Fig. 1, open squares). Components of absorption and the normalized absorption spectra were measured as described previously (Gallegos and Neale, 2002). Here we present measurements of absorption by CDOM at 440 nm [i.e. $a_g(440)$] as an independent check on values estimated by inversion of monitored ac9 data (Gallegos and Neale, 2002, see Appendix A), and for delineating spatial gradients as an indication of CDOM sources.

3.5. Supporting measurements

To gain insight into the processes governing seasonal variations in optical properties, we compared patterns of variation in optical properties with various long-term measurements of parameters capable of influencing CDOM, phytoplankton, and total suspended solids (TSS). We measured the concentration of TSS in a series of transects of the Rhode River and Muddy Creek at approximately bi-weekly intervals from 1986 to 2001. The concentration of TSS was determined from the weight gain of a pre-weighed, 0.45 μm Poretics filter. Additionally, during 2000 and 2001 we determined the fraction of combustible suspended solids by filtering samples through a pre-combusted GF/F glass fiber filter, and determining the dry-weight loss after combustion for 3 h at 500 °C. Methods of sample collection and data through 1989 are reported in Jordan et al. (1991). Concentrations of NO_3, NH_4, and PO_4 in samples from the bi-weekly transects were measured by previously published methods (Jordan et al., 1991). Data shown here were from the transect segment closest the optical monitoring station (Fig. 1, dotted line).

Discharge from 36% of the watershed of Muddy Creek was monitored from 1985 to 1999 with a network of weirs and automated samplers. Location of the

automated samplers is given in Gallegos et al. (1992). Flow was measured at V-notch weirs, and samples in volumes proportional to the flow were pumped into acid-washed glass carboys (Correll, 1981; Correll et al., 1999). Samples were composited weekly and analyzed for TSS concentration as described above. These data provided an estimate of the seasonal pattern of weekly mean suspended sediment influx from the local watershed (Jordan et al., 1986).

We estimated the contribution of living plankton to the organic fraction of TSS from long-term measurements of phytoplankton chlorophyll and ciliate abundance. Vertically integrated water samples were collected from a station ca. 100 m from the monitoring pier using a 2-l Labline Teflon sampler by slowly lowering and raising the sampler in less time than required to fill the sampler. Samples for chlorophyll analysis (1990–2001) were filtered onto Whatman GF/F glass fiber filters, extracted in 10 ml of 90% acetone overnight at 4 °C either immediately or after freezing for <2 week. We estimated the dry weight of phytoplankton by assuming a carbon-to-chlorophyll ratio of 40 mg C (mg Chl)$^{-1}$ (Gallegos, 2001) and a dry weight-to-carbon ratio of 3.33 mg dry weight (mg C)$^{-1}$ based on Redfield elemental composition. Samples for ciliate counting (1992–1994) were preserved in modified Bouin's fixative (Coats and Heinbokel, 1982) and processed by the quantitative protargol staining (QPS) technique of Montagnes and Lynn (1993). Ciliate abundances were derived from 25–50 ml QPS preparations by enumerating specimens present in arbitrarily selected microscope fields (×1250) until a total of 100 individuals or the equivalent of 2 ml of whole-water sample was counted. Ciliates were classified by morphotypes, with genus and species identifications made whenever possible. Length and width measurements were obtained for each morphotype using a calibrated ocular micrometer. For common ciliate taxa, five length-width determinations were made per sample until ≥100 measurements were obtained. Uncommon taxa were sized when encountered (10–50 estimates per morphotype); however, <10 measurements were obtained for rare morphotypes. Species-specific biovolumes were calculated from QPS dimensions using appropriate geometric formulae. For each sample, species abundance and biovolume were multiplied, and resultant values summed across morphotypes to give cumulative biovolumes for total ciliates. Cumulative biovolumes were converted to carbon biomass using a factor of 0.27 pg C μm^{-3} for protargol stained specimens (Bockstahler and Coats, 1993), and to dry weight by a factor of 2.11 g dry weight (g C)$^{-1}$ based on Fenchel and Finlay (1983).

As an indicator of the potential for bioturbation to influence TSS concentrations, we examined the monthly averaged biomass of epibenthic fish and crabs in the Rhode River. Abundances of epibenthic fish and crabs were estimated with otter trawls from 1981 to 2002 by procedures of Hines et al. (1990). For each trawl (Fig. 1, arrows), all organisms caught were counted and identified to species. Body sizes (total body length of fish and maximal carapace width of blue crabs) of a subset of 20 individuals were randomly selected for measurement; all individuals were measured when total catch of a species was <20 individuals. Biomass as wet weight was calculated from established regressions against length (Dawson, 1965 for fish; Olmi and Bishop, 1983 for crabs), and expressed as kg trawl^{-1}. Analysis was restricted to the most consistently observed mobile bottom feeding taxa, namely blue crabs (*Callinectes sapidus*), and demersal fish mainly composed of spot (*Leiostomus xanthurus*), and croaker (*Micropogonias undulatus*).

4. Results

4.1. Monitoring efficiency

Data from the monitoring system consist of 10,534 measurements of spectral absorption and attenuation coefficients measured from January 2000 through September 2001. Excluding days that the system was not operated due to the threat of ice (91 days between the two winters), gross efficiency of data collection was approximately 80%. Data loss occurred due to a combination of occasional recorder failure, loss of power, and 431 measured spectra were rejected due to entrainment of bubbles or accumulation of particulate matter, which were recognized by high and erratic spectra that produced unrealistic estimates of absorption components. The data show a high degree of variability on nearly every time scale. Therefore we calculated weekly averages for better resolution of seasonal and interannual patterns. Shorter-term variability will be examined in another paper.

4.2. Absorption spectra

Weekly averages of total absorption coefficient at 440 nm and the magnitudes of the components comprising it underwent a similar pattern of variation in each year (Fig. 2a and Fig. 3a). There was a minimum for all components in late winter, a noticeable spring phytoplankton bloom (ca. day 120), a decline in all components following the collapse of the spring bloom (ca. day 150), a gradual build up of non-algal particulate absorption for the remainder of the summer, and a rapid decline of all components in late summer, ca. day 270 (only measured in 2000).

Absorption by CDOM was the least variable absorption component, varying from about 0.3 m^{-1} in winter to about 1 m^{-1} in summer (Fig. 2a). There was a tendency

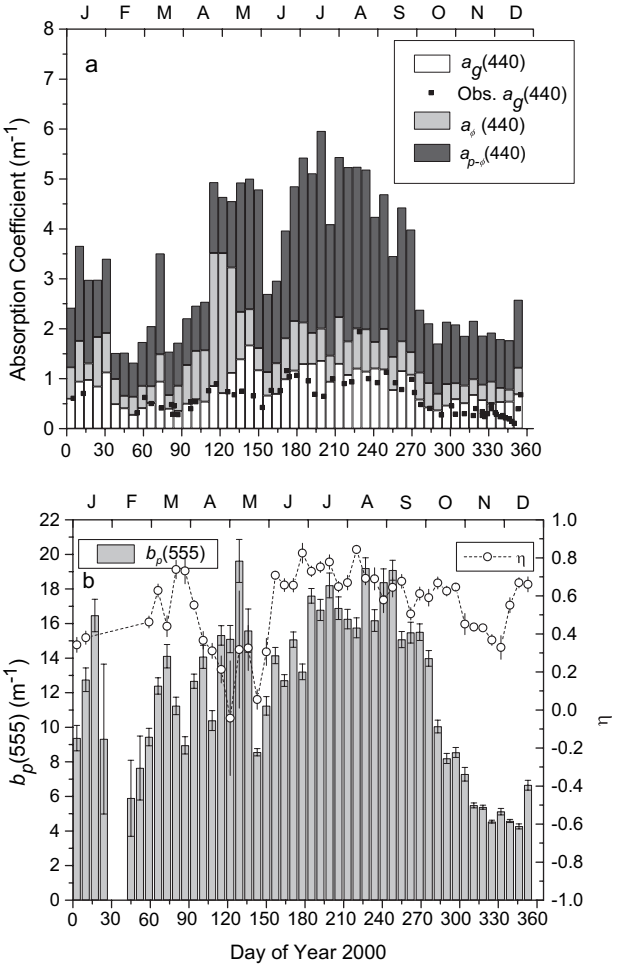

Fig. 2. (a) Weekly averages of components of absorption at 440 nm in the Rhode River estimated from monitored absorption and attenuation spectra in 2000. White bars—absorption by CDOM; gray bars—absorption by phytoplankton; black bars—absorption by non-algal particulates. Small squares are absorption by CDOM, a_g(440), measured on grab samples. (b) Weekly averages of scattering coefficients at 555 nm (gray bars) in the Rhode River, and weekly averages of the spectral exponent, η, characterizing the spectral variability in scattering coefficients (open circles) for 2000. Error bars are of 95% confidence limits.

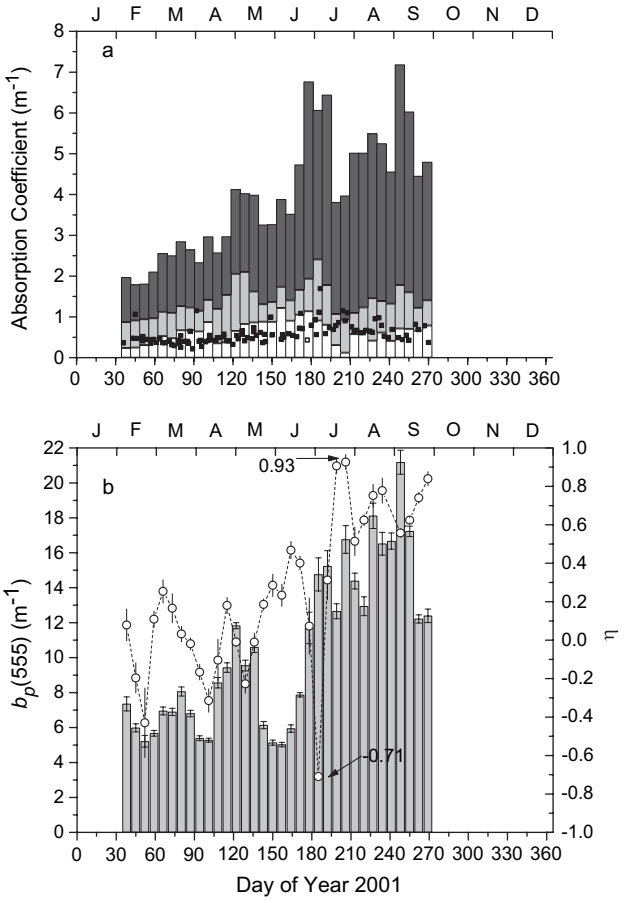

Fig. 3. As Fig. 2 for year 2001. Arrows and numbers designate points chosen to demonstrate differences in scattering spectrum with different exponents (see Fig. 4).

for the inversion algorithm to overestimate a_g(440), though the overall seasonal pattern was well resolved in 2000. Due to the inability to predict the absorption-to-scattering ratio (ρ) exactly (see Appendix A), there is an unavoidable tendency for estimates of a_g(440) to covary with estimated $a_{p-\phi}$(440) (Fig. 2a and Fig. 3a, see also Gallegos and Neale, 2002). This covariation between estimates of a_g(440) and $a_{p-\phi}$(440) resulted in, for example, overestimates of a_g(440) following the spring phytoplankton bloom in 2000 (Fig. 2a, days 135–150) and underestimate a_g(440) after a fall phytoplankton bloom in 2001 (Fig. 3a, days 195–210).

The spring phytoplankton bloom was much larger in 2000 than in 2001, but in each year there was an increase in absorption in non-algal particulate matter at the termination of the bloom that kept total absorption coefficient at bloom levels for longer than that due to the phytoplankton bloom alone (Gallegos and Jordan, 2002).

The relative minimum in the sum of absorption components in early summer, ca. day 160, following the collapse of the bloom was much more noticeable in 2000 than in 2001, due to the much larger bloom that year. Nevertheless, such a decline that also occurred in 2001 is borne out by measurements of scattering coefficients (see below).

4.3. Scattering coefficients

The seasonal pattern of scattering coefficient at 555 nm (Fig. 2b and Fig. 3b) was similar to that of absorption by non-algal particulate matter. There was a relative peak near the end of the spring phytoplankton bloom (ca. day 135), a relative minimum near day 150 that was particularly evident in 2001, a gradual rise to a seasonal maximum in late summer (ca. day 240), and a rapid decline in fall (after day 270, only measured in 2000). Scattering coefficients were higher in 2000 than in

2001, until about mid-summer (i.e. day 200, Fig. 2b and Fig. 3b).

The spectral exponent of scattering, η, varied widely within and between years (Fig. 2b and Fig. 3b). In 2000 (Fig. 2b, open circles) there appeared to be a trend characterized by relatively high values in early spring soon after the breakup of ice (ca. days 60–90), declines during the bloom of *Prorocentrum minimum* (days 110–150), followed by a steady rise after day 150 to a late summer peak. The most consistent feature between the 2 years was the relatively high values in late summer (days 200–270). The relatively low values during the smaller spring bloom of *P. minimum* from ca. days 110–150 in 2001 were similar to those in 2000, but were not as clearly associated with the bloom due to other low values early in the year (Fig. 3b). The rise to the late summer maximum in 2001 was interrupted by a sudden decline to the lowest weekly averaged value observed in the data set at about day 185. Examination of ancillary data (Gallegos, unpublished) indicated that this time period corresponded to a modest bloom of the small dinoflagellate *Karlodinium micrum* cf. of about 10^4 cells ml^{-1}, representing about a three-fold increase in chlorophyll from about 15 to 45 mg m^{-3}. The largest absorption due to phytoplankton observed during 2001 also occurred during this week (cf. Fig. 3a, ca. day 185). Within 2 weeks the averaged η had returned to values >0.6 (Fig. 3b), characteristic of late summer conditions seen in 2000.

Examples of scattering spectra with low (−0.71) and high (0.93) values of η are given in Fig. 4. Depression of scattering in the chlorophyll absorption bands in the blue (412–488 nm) and the red (676 nm) was evident in the spectrum with the low η (Fig. 4, filled squares), indicating a noticeable effect of phytoplankton absorption (Stramski and Mobley, 1997). The spectrum with the large η (Fig. 4, open circles) decreased monotonically with increasing wavelength, indicating dominance of the scattering by smaller plankton or mineral particulates (Babin et al., 2001).

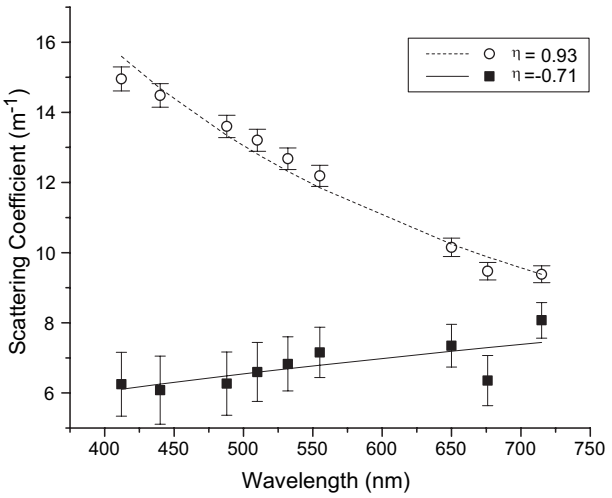

Fig. 4. Model fits to weekly averaged scattering spectra representing the highest (open circles and dashed line, $\eta = 0.93$) and lowest (filled squares and solid line, $\eta = -0.71$) spectral exponents estimated in the time series. In the case of low η, the model does not fit the depression of scattering observed in chlorophyll absorption bands, especially at 676 nm.

4.4. Sources of materials and environmental covariates

Seasonal changes in the parameters that determine optical properties are examined in relation to driving processes for 2000, the year of more complete measurements. Sources of CDOM include stream and groundwater inputs from the local watershed and wetlands of Muddy Creek, phytoplankton excretion and lysis, and benthic decomposition of settled phytoplankton and organic matter. Sinks for CDOM include bacterial and photo-degradation. Exchange at the mouth with Chesapeake Bay may be either a source or sink, depending on the direction of the gradient.

The potential for freshwater inputs of CDOM peaked during the months of March through May when discharge from both the local watershed of Muddy Creek and from the Susquehanna River (the main freshwater source to upper Chesapeake Bay) was sustained at high levels (Fig. 5a). If freshwater inputs were the main source of CDOM, then we would expect CDOM absorption to vary inversely with salinity. However, salinity was not a good correlate of CDOM absorption, because salinity reached a minimum (ca. day 120) and increased steadily for most of the remainder of the year (Fig. 5b, filled squares), while CDOM absorption increased irregularly to ca. day 270, then declined abruptly while salinity continued to increase (cf. Fig. 5b and c).

The overall seasonal pattern of CDOM absorption followed that of temperature (cf. Fig. 5b and c), especially in regard to the rapid decline in fall. Spatial patterns varied seasonally, with minimal spatial gradients in spring (with the exception of elevated concentrations at the mudflat station due to local flow ca. day 80) and late fall, and pronounced spatial gradients from late spring through late summer (Fig. 5c). Only in late winter (ca. day 60) during peak flow of the Susquehanna River and in late spring (ca. day 150) following the collapse of the widespread bloom of *Prorocentrum minimum* (Gallegos and Jordan, 2002) did CDOM absorption at the mouth of the Rhode River exceed that at up-estuary stations (Fig. 5c). Otherwise CDOM absorption increased in the up-estuary direction. It would thus appear that in situ production of CDOM dominated the seasonal signal, with production rates increasing up-estuary parallel with the overall trophic gradient in the system (Jordan et al., 1991).

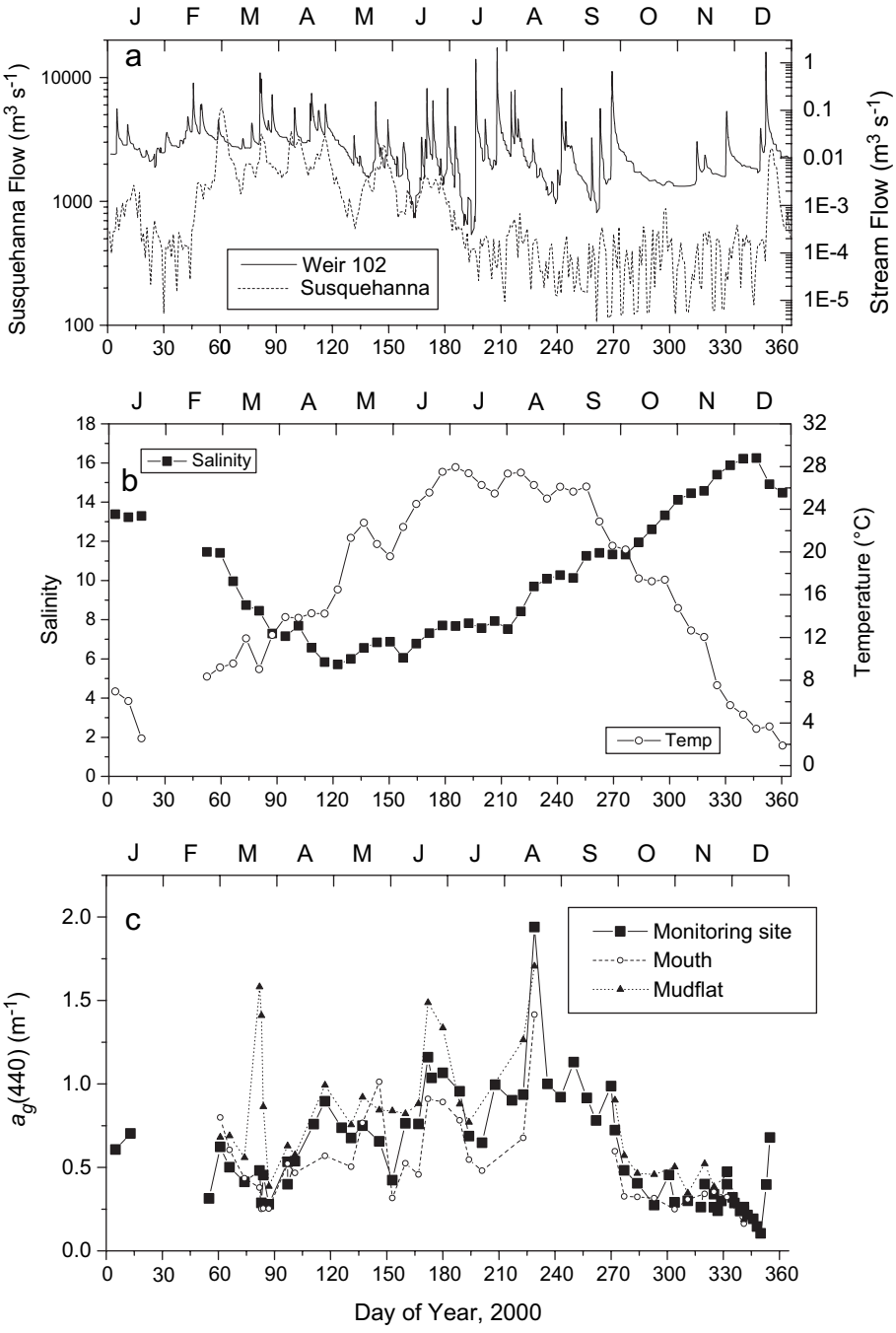

Fig. 5. Time series of the measured concentration of CDOM and potential environmental correlates for year 2000: (a) freshwater flow by (solid line) the North Branch of Muddy Creek measured at weir 102, and (dotted line) the Susquehanna River, main freshwater source for northern Chesapeake Bay; (b) salinity (filled squares) and temperature (open circles); (c) concentration of CDOM measured in grab samples from different locations (see Fig. 1) along the axis of the estuary, (filled squares) the monitoring site, (open circles) mouth of the Rhode River, and (filled triangle) the subtidal mudflats (up-estuary).

Absorption by phytoplankton at 676 nm as estimated from the monitoring data closely paralleled changes in extracted chlorophyll (Fig. 6a). The seasonal variability in chlorophyll absorption was dominated by the extraordinary spring bloom of *Prorocentrum minimum*, described previously by Gallegos and Jordan (2002), who observed the onset of the bloom in response to the freshet of the Susquehanna River. A brief spike in measured nitrate concentration to >12 μM can be seen prior to the spring bloom (Fig. 6b), with concentrations remaining mostly below 4 μM the remainder of the year. Variations in chlorophyll absorption (or chlorophyll concentration) bore no obvious relationship with any other measured nutrient (cf. Fig. 6a and b).

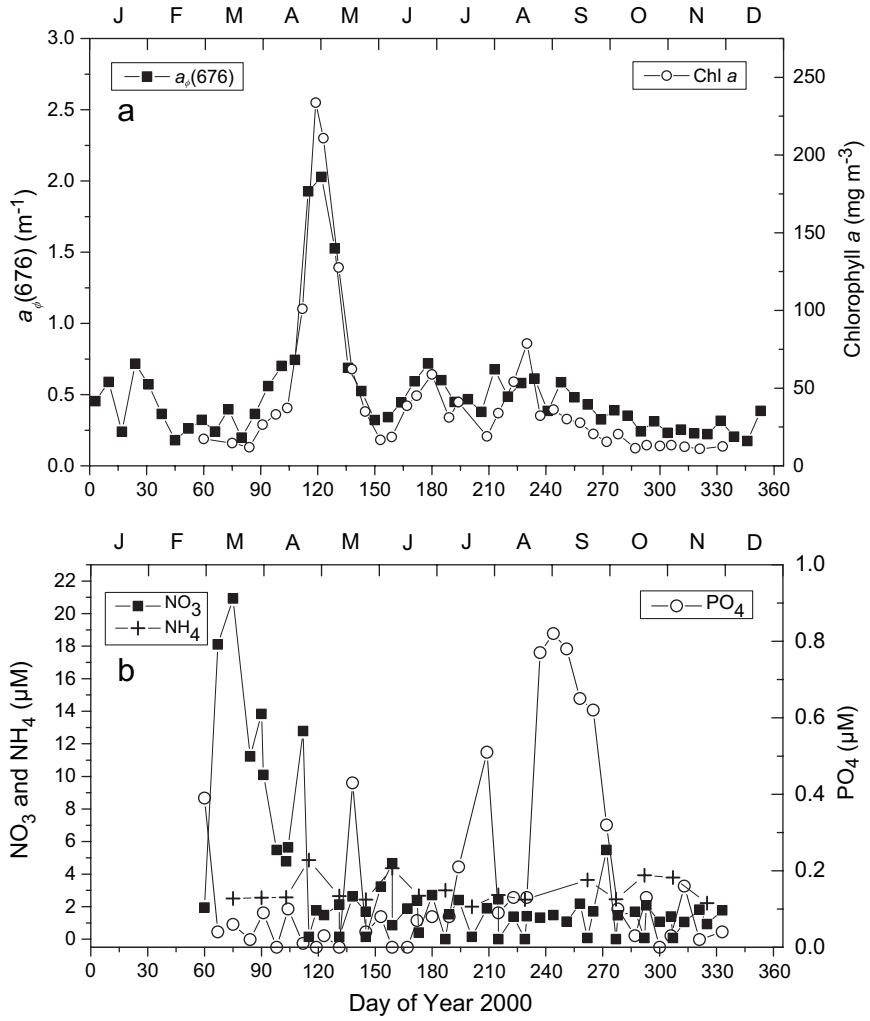

Fig. 6. Weekly averages of measured absorption by phytoplankton at 676 nm and potential environmental correlates for the year 2000: (a) comparison of (filled squares) measured $a_\phi(676)$ with (open circles) measured chlorophyll concentration, and (b) measured concentrations of macronutrients, (filled squares) nitrate, (plus signs) ammonium, and (open circles) phosphate.

Absorption by non-algal particulate matter was higher and more variable in late winter, i.e. days 1–75, than in early winter (day 300–360) due to intermittent disturbance of the shoreline by tidal movement of ice (Fig. 7a). Samples collected at these times of ice movement were grab samples taken off the end of the dock where the ac9 was housed, since the monitor could not be run under those conditions. Non-algal particulate absorption at 440 nm increased from about 1 m^{-1} during late spring to $>3\ m^{-1}$ at the termination of the spring bloom of *Prorocentrum minimum*, declined near day 150, then rose steadily to a mid- to late summer maximum, and declined rapidly in the fall back to ca. 1 m^{-1} (Fig. 7a). The seasonal trend corresponded only weakly to the variation in concentration of total suspended solids (TSS), due to the extremely high concentration of TSS measured during the spring bloom (Fig. 7b). The partitioning inversion correctly attributed the absorption by the spring bloom to phytoplankton (Fig. 6a). Otherwise, TSS concentration rose to a local peak in late summer (ca. day 220) and declined steadily in the fall, similar to absorption by non-algal particulate matter.

The overall seasonal trend in scattering coefficient (Fig. 7a, open circles) corresponded better with TSS concentration than did $a_{p-\phi}(440)$, including the peak in TSS concentration that occurred due to the spring phytoplankton bloom. Nevertheless, the late summer relative maxima and fall declines in both scattering coefficients and absorption by non-algal particulates appeared to be governed by the variation of TSS (Fig. 7).

4.5. Comparisons with long-term determinants of TSS

We examined average seasonal patterns in various long-term data from the Rhode River system to try to determine causal mechanisms regulating concentrations of non-algal particulate matter. The average weekly

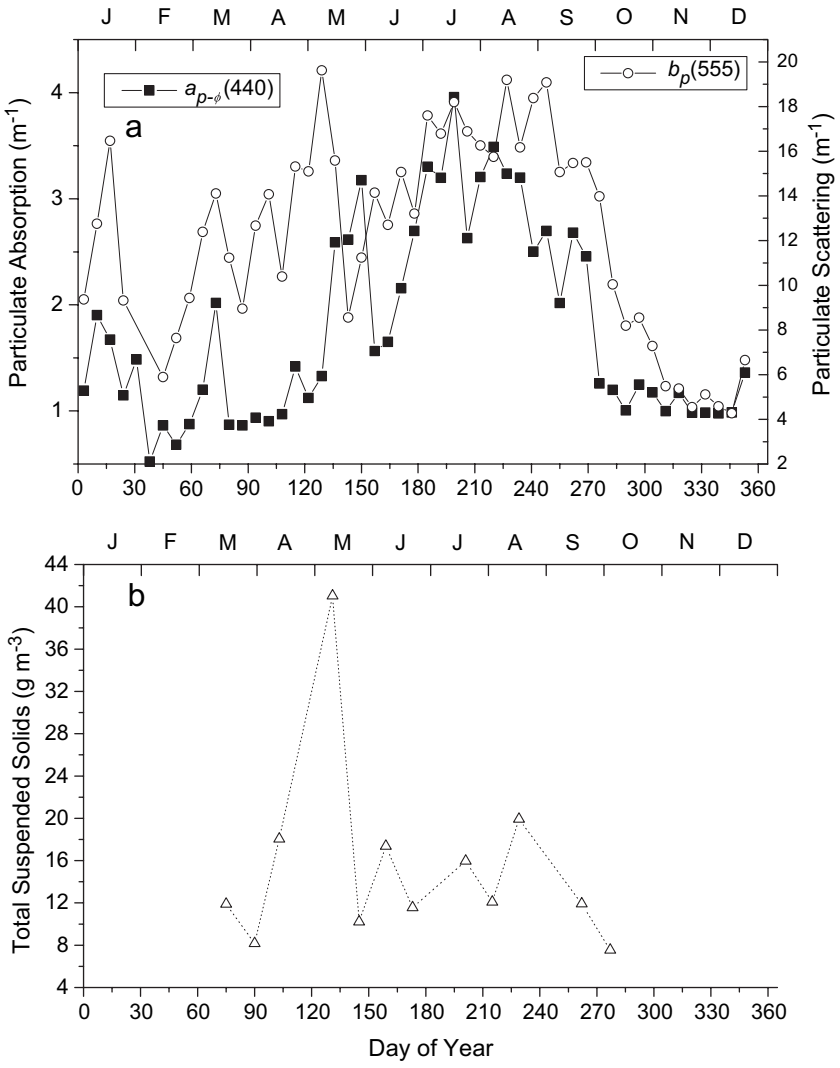

Fig. 7. Weekly averages of (a) absorption by non-algal particulates, and (b) time series of suspended particulate matter concentration measured in independent transect cruises for the year 2000. Large peak in TSS concentration in spring was due to the spring dinoflagellate bloom, and precedes a peak in non-algal particulate absorption.

concentration of TSS in long-term data from the region around the monitoring station on the Rhode River has peaks in spring corresponding with the average timing of the spring phytoplankton bloom, and in late summer (Fig. 8a, squares) coinciding with the timing of the late summer maximum in $a_{p-\phi}(440)$ and scattering coefficient (Fig. 7). The fraction of TSS that is not combustible at 500 °C varied between 0.5 and 0.8, and seemed to be only slightly lower during the phytoplankton growing season from days 120 to 270 than during other times (Fig. 8a, thin line). Consequently, estimates of the organic and inorganic fractions of TSS exhibit similar seasonal patterns (Fig. 8b and c). The seasonal pattern of estimated dry weight of phytoplankton plus ciliates follows the overall trend of the estimated organic solids, and, excepting the overestimate of the phytoplankton contribution to dry weight during the spring bloom, quantitatively accounts for a large proportion of the organic solids concentration (Fig. 8b). Ciliate biomass only adds noticeably to the dry weight of phytoplankton during mid-summer. The primary difference between the patterns of inorganic and organic suspended solids is the presence of a broad peak in inorganic suspended solids in early spring coinciding with maximal watershed inputs and seasonal mean windspeed (Fig. 8c).

The overall similarity of both the combustible and the non-combustible fractions of TSS to the annual temperature cycle (cf. Figs. 8 and 5b), resulting in a mid-summer peak that is out of phase with watershed delivery and windspeed, strongly suggests a dependence of TSS concentration on biological activity. Not surprisingly, therefore, the mid-summer peak of TSS and its rapid decline in the fall parallel the long-term average biomass of mobile benthic predators such as *Calinectes sapidus* (blue crabs) and a variety of fish

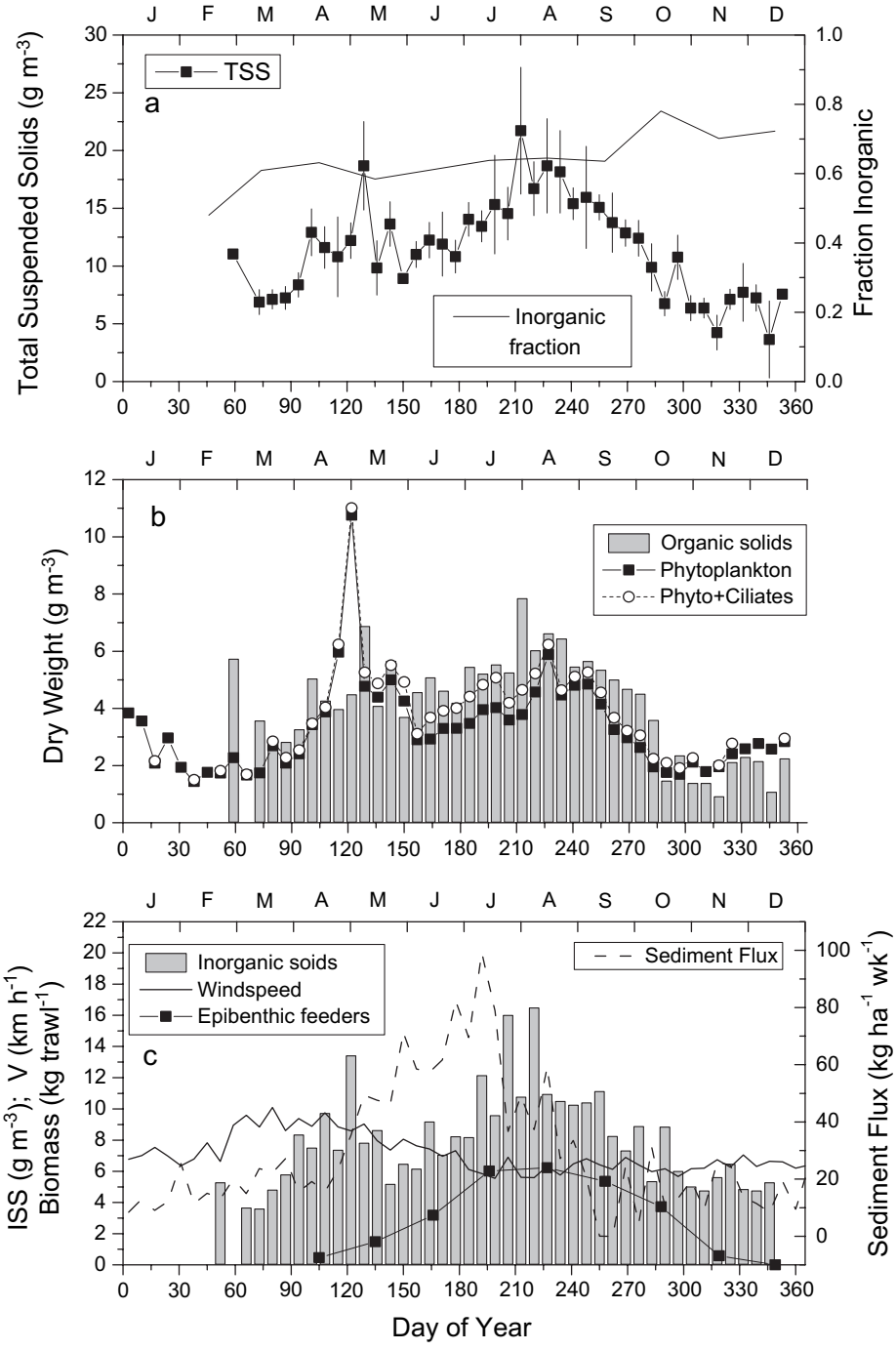

Fig. 8. Time series of weekly (unless otherwise specified) medians of long-term measurements of suspended particulate matter and related parameters considered potential drivers of the average seasonal pattern. (a) Concentration of (squares) total suspended particulate matter, and (thin line) fraction of TSS that is inorganic (monthly data). Error bars are ± 1 standard error; (b) dry weight of (filled squares) phytoplankton estimated from chlorophyll concentration and (open circles) phytoplankton plus ciliates, compared with (gray bars) estimated organic fraction of TSS. Ciliates add measurably to total dry weight in mid-summer. Sum of phytoplankton and ciliates accounts for most of the variation in organic suspended solids; (c) seasonal pattern of (gray bars) estimated inorganic component of TSS compared with factors that input or resuspend inorganic sediments—(bold line) windspeed, (bold dashed line) watershed influx from streamflow, and (thin line and squares) biomass of epibenthic predators (monthly data). Epibenthic predators consist mainly of croaker (*Micropogonias undulates*, ca. 2–3% of summer peak), spot (*Leiostomus xanthurus*, ca. 20% of summer peak), and blue crabs (*Callinectes sapidus*, ca. 76–78% of summer peak).

(Fig. 8c, squares) which could contribute to sediment resuspension by their feeding activity.

5. Discussion

Together the phytoplankton and non-algal particulate matter dominated the variability in optically active constituents in the Rhode River (Figs. 2 and 3). Interannual variability in the magnitude of the spring phytoplankton bloom was pronounced—the 2 years observed here included blooms of extraordinary (2000) and average (2001) magnitudes for this system (Gallegos et al., 1997). Modeling studies (Gallegos et al., 1997) and detailed automated monitoring data (Gallegos and Jordan, 2002) have shown that interannual variability in the magnitude of the spring bloom in the Rhode River is governed by the timing and magnitude of nitrate inputs by the spring freshet of the Susquehanna River. The freshet must be large enough to carry high concentrations of nitrate, must not arrive prior to adequate daylength and seasonal phosphate availability (i.e. after mid-March), or so late that the nitrate is consumed during its transit along the axis of northern Chesapeake Bay (i.e. before mid-May) (Gallegos et al., 1997; Gallegos and Jordan, 2002).

Absorption by CDOM in summer 2000 also exceeded that in 2001 (Fig. 2a and Fig. 3a). If the interannual difference in CDOM absorption was related to the differences in relative magnitudes of the spring phytoplankton blooms, then the increase took longer to be expressed than the absorption by non-algal particulates. The observations are consistent with death of autotrophs and growth of heterotrophic plankton producing the peak in non-algal absorption following bloom collapse, and longer-term decomposition over the summer producing the higher levels of absorption by CDOM. The lack of correlation between CDOM absorption and salinity differs from some studies that have examined spatial gradients in coastal systems in individual cruises (Twardowski and Donaghay, 2001; Hu et al., 2003). However, because the Rhode River is a subestuary, salinity at the mouth varied from ca. 5 to 16 over the observation period (similar to that at the monitoring site, Fig. 5b). Within this restricted salinity range, Harding et al. (2005) observed CDOM absorption in the main stem of Chesapeake Bay varying from 0.3 to 0.8 m^{-1}, and only weakly correlated with salinity. Similarly, CDOM absorption of local stream flow varied from <0.5 to >3 m^{-1} (Gallegos, unpublished), so that weak correlation between CDOM absorption and salinity on seasonal time scales is not unexpected. Gallegos (2005) observed similar lack of correlation between salinity and CDOM absorption in the humic-stained St. Johns River, due primarily to large spatial and temporal variations in CDOM absorption at zero-salinity within the tidal freshwater portion of the estuary.

The interannual variability in non-algal particulate matter appeared less pronounced than that of phytoplankton, except for the peak in non-algal particulate absorption associated with the collapse of the extraordinary spring phytoplankton bloom in 2000 which was not observed in 2001. The mid- to late summer peaks in scattering coefficient and non-algal particulate absorption, as well as the fall declines were similar in the 2 years (Fig. 2b and Fig. 3b). The late summer increase in spectral exponent of scattering (Fig. 2b and Fig. 3b) indicates a decrease in the particle-size spectrum consistent with known seasonal shifts in species composition from diatoms to picoplankton and flagellates in Chesapeake Bay (Malone et al., 1996), and/or increasing mineral contribution to scattering (Babin et al., 2003).

As was observed on the continental shelf of the Middle Atlantic Bight (Chang and Dickey, 2001), much of the variability in optical properties in the Rhode River subestuary was related to season. By examining weekly averages of optical properties, we removed much of the variability in our data associated with short-term episodic events that characterized the observations of Chang and Dickey (2001) on the continental shelf. In this study, however, we were also able to observe interannual variability, which was pronounced with respect to the magnitude of the spring phytoplankton bloom and its collapse. The contrasting years help us resolve variability that was directly related to phytoplankton blooms from that which was not. Aside from the differences in the magnitude of phytoplankton absorption, the largest difference between the 2 years was the pronounced peak in absorption by non-algal particulates as the extraordinary bloom collapsed in 2000, which was missing in 2001. Gallegos and Jordan (2002) showed that the increase in non-algal absorption in 2000 initially coincided with a transient increase in empty thecae of *Prorocentrum minimum*, indicating that cell mortality was a likely factor at first. Growth of bacteria and other heterotrophic plankton may have sustained the peak in non-algal absorption. The observation that the late summer maximum in non-algal particulate absorption (Fig. 2a and Fig. 3a) and scattering coefficient (Fig. 2a and Fig. 3a) were similar between the 2 years indicates that the formation of the late summer maximum in particulate matter does not depend upon having an extraordinary phytoplankton bloom in the spring.

The late summer peak in absorption by non-algal particulate matter appeared to have a biological explanation (Fig. 8c). As is common in many low energy coastal systems (Pempkowiak et al., 2002), a benthic fluff layer forms on the bottom of the Rhode River in the region of the optical monitoring station, and is especially pronounced during the summer. Where they have been studied, such layers have been shown to be

highly fluidized (Amos et al., 1997), composed of a mixture of sedimented phytoplankton (Beaulieu, 2003), protists (Shimeta et al., 2002), and fine sediment (Pempkowiak et al., 2002), and resuspended much more easily than consolidated sediments of similar composition (Maa et al., 1998; Leipe et al., 2000). Increased erodability of this material even under the reduced winds of summer might be sufficient to produce the mid-summer peak in TSS concentration. Hines et al. (1990) demonstrated that bioturbation by the epibenthic predatory guild of blue crabs and fish disturbed the top layer of benthic sediments to a depth of 10 cm at a station in the Rhode River during summer. The activity of these organisms may, therefore, interact with wind and tidal resuspension to produce the mid-summer peak in both organic and inorganic suspended particulate matter. Biological activity was also shown to be a factor in resuspension of a benthic fluff layer that varied in amount with season and location in lower Chesapeake Bay (Maa and Lee, 1997). Similarly, epibenthic fish were shown to facilitate sediment resuspension, while experimental removal of fish promoted bottom sediment consolidation in a shallow lake in the Netherlands (Scheffer et al., 2003).

Additionally, seasonal formation of the benthic fluff layer may, in part, rely on particle flocculation and sedimentation of flocs from the water column. Though salt flocculation of charged primary clay particles is rapid, formation of macroflocs consisting of coated minerals and detritus is enhanced by polysaccharides and polymers produced by bacteria (van Leussen, 1988). Such a process might scavenge the water column of particles as temperature rises and the spring bloom collapses in late spring (Jones et al., 1998), possibly accounting for the late spring minimum in inorganic suspended solids (Fig. 8c) and scattering coefficients (Fig. 2b, Fig. 3b and Fig. 7) around day 150.

These results have implications for the development of indicators of water quality and habitat suitability for living resources in the coastal zone. Gallegos and Jordan (2002) demonstrated that absorption and scattering by non-algal particulate matter extended the impact of an extraordinary dinoflagellate bloom on light attenuation an additional 2 weeks longer than that due to phytoplankton alone. Furthermore, if we are correct that biotic resuspension of a phytodetritus and sediment fluff layer is responsible for the late summer maximum in attenuation, then it is clear that eutrophication has long-term effects on optical properties of a water body beyond the immediate absorption and scattering of light directly attributable to phytoplankton. Neither chlorophyll concentration nor phytoplankton species composition provides a measure of this aspect of eutrophication. Finally, the independence of this process from the magnitude of the preceding spring bloom indicates that the effects of eutrophication on optical properties of the non-algal particulate matter may take multiple years to reverse.

Acknowledgments

Support for this work was provided by the U.S. Environmental Protection Agency through the Coastal Intensive Site Network (CISNet) grant R826943 and the Estuary and Great Lakes Coastal Initiative (EaGLes) grant R82868401, and by the Smithsonian Environmental Sciences Program. The research described in this paper has not been subjected to the U.S. Environmental Agency's required peer and policy review and therefore does not necessarily reflect the views of the Agency and no official endorsement should be inferred. We thank D.W. Coats for data on ciliate biovolume, and K. Yee, D. Sparks, J. Miklas, and R. Aguilar for help with data collection and analyses.

Appendix A

The ac9 measures absorption coefficients referenced to the absorption by pure water, which is subtracted by the manufacturer's software. In addition, the measured coefficients overestimate true absorption due to loss of photons by scattering within the reflective tube, which the instrument incorrectly attributes to absorption (Kirk, 1992). Kirk (1992) demonstrated that, for a given scattering phase function, the error is proportional to the scattering coefficient, which can be used to derive a correction factor (Zaneveld et al., 1994; Gallegos and Neale, 2002),

$$a_{t-w}(\lambda) = a_m(\lambda) - \varepsilon[c(\lambda) - a_m(\lambda)] = a_m(\lambda) - \varepsilon b_m(\lambda) \quad \text{(A1)}$$

where λ is the wavelength of light, $a_{t-w}(\lambda)$ is the true total absorption less that due to water, $a_m(\lambda)$ is the absorption coefficient measured by the ac9, $c(\lambda)$ is the attenuation coefficient, $b_m(\lambda) \equiv c(\lambda) - a_m(\lambda)$ is the measured scattering coefficient, and ε is a correction factor. We estimated ε by the procedure of Gallegos and Neale (2002) using their unconstrained matrix inversion. Note that $b_m(\lambda)$ underestimates the true particulate scattering, $b_p(\lambda)$, by the factor $(1 + \varepsilon)$.

We estimated the components of absorption by a modification of the procedure of Gallegos and Neale (2002). We represented the absorption coefficient referenced to water as the sum of absorption due to colored dissolved organic matter (CDOM), phytoplankton pigments, and non-algal particulate matter,

$$a_{t-w}(\lambda) = a_g(\lambda) + a_\phi(\lambda) + a_{p-\phi}(\lambda) \quad \text{(A2)}$$

where the subscripts refer to absorption by particular components: g for CDOM (i.e. *gelbstoff*, Kirk, 1994),

ϕ for phytoplankton, and $p-\phi$ for non-algal particulate matter. The component absorption spectra were represented by normalized absorption functions, scaled by the absorption at a characteristic wavelength,

$$a_g(\lambda)=a_g(440)g(\lambda) \tag{A3a}$$

$$a_\phi(\lambda)=a_\phi(676)\phi(\lambda) \tag{A3b}$$

and

$$a_{p-\phi}(\lambda)=a_{p-\phi}(440)p(\lambda) \tag{A3c}$$

where $g(\lambda)$, $\phi(\lambda)$, and $p(\lambda)$ are the normalized absorption functions for, respectively, CDOM, phytoplankton, and non-algal particulate matter. Substituting Eqs. (A3a)–(A3c) into Eq. (A2) and equating to the right hand side of Eq. (A1) produces a linear system of equations with 4 unknowns consisting of the scale factors in Eqs. (A3a)–(A3c) and ε, measurements $a_m(\lambda)$ and $b_m(\lambda)$, and coefficients given by the normalized absorption spectra. The system is fully determined using measurements at 4 wavelengths, so that the scale factors and ε may be determined by matrix inversion. Gallegos and Neale (2002) called this procedure the unconstrained solution.

The unconstrained solution performed well for estimating $a_\phi(676)$ and ε, but sometimes produced unstable estimates of $a_g(440)$ and $a_{p-\phi}(440)$, due to the similar shapes for $g(\lambda)$ and $p(\lambda)$. Gallegos and Neale (2002) used a statistically augmented procedure to improve the discrimination between absorption by CDOM from that by non-algal particulates, by noting that non-algal particulate matter contributes to scattering, whereas CDOM does not. They parameterized the scale factor for absorption by non-algal particulates in terms of the absorption-to-scattering ratio of non-algal particulates at 440 nm, ρ, where

$$\rho\equiv\frac{a_{p-\phi}(440)}{b_p(440)} \tag{A4}$$

and estimated ρ by a site-specific statistical model. However, over or underestimates of ρ could still produce negative estimates of $a_g(440)$ or $a_{p-\phi}(440)$. Here we further modified the procedure by noting that ρ must lie along the line,

$$\rho=\rho_{cm}(1-f_c) \tag{A5}$$

where $\rho_{cm}=\left(a_{p-\phi}(440)+a_g(440)\right)/b_p(440)$ is the absorption-to-scattering ratio of particulate plus dissolved matter and is fixed by the measurements once ε and $a_\phi(676)$ have been estimated, and $f_c=a_g(440)/\left(a_{p-\phi}(440)+a_g(440)\right)$ is the fraction of total non-algal absorption at 440 nm attributable to CDOM. We used the statistically augmented procedure of Gallegos and Neale (2002) to provide a first estimate of $\hat{\rho}$, $\hat{a}_g(440)$, and $\hat{f}_c$, then revised the estimate by finding the nearest point on Eq. (A5) that was also on the normal to Eq. (A5), passing through $(\hat{f}_c,\ \hat{\rho})$. The revised procedure guarantees positive estimates for $a_g(440)$ and ρ whenever measured spectra conform to the shape predicted by Eqs. (A2), (A3a)–(A3c). Note that, though the procedure only estimates 3 scale coefficients at a characteristic wavelength, the procedure exploits the spectral variability in absorption at 4 widely spaced wavelengths. The complete spectral shape of absorption is implied by the scale factors applied to the normalized absorption functions. It is, of course, not possible to simultaneously estimate the scale factors and the normalized absorption functions.

References

Aksnes, D.L., Nejstgaard, J., Soedberg, E., Sørnes, T., 2004. Optical control of fish and zooplankton populations. Limnology and Oceanography 49, 233–238.

Amos, C.L., Feeney, T., Sutherland, T.F., Luternauer, J.L., 1997. The stability of fine-grained sediments from the Fraser River Delta. Estuarine, Coastal and Shelf Science 45, 507–524.

Babin, M., Morel, A., Fournier-Sicre, V., Fell, F., Stramski, D., 2003. Light scattering properties of marine particles in coastal and open ocean waters as related to the particle mass concentration. Limnology and Oceanography 48, 843–859.

Beaulieu, S.E., 2003. Resuspension of phytodetritus from the sea floor: a laboratory flume study. Limnology and Oceanography 48, 1235–1244.

Bockstahler, K.R., Coats, D.W., 1993. Grazing of the mixotrophic dinoflagellate Gymnodinium sanguineum on ciliate populations of Chesapeake Bay. Marine Biology 116, 477–487.

Chang, G.C., Dickey, T.D., 1999. Partitioning in situ total spectral absorption by use of moored spectral absorption–attenuation meters. Applied Optics 38, 3876–3887.

Chang, G.C., Dickey, T.D., 2001. Optical and physical variability on timescales from minutes to the seasonal cycle on the New England shelf: July 1996 to June 1997. Journal of Geophysical Research 106, 9434–9453.

Coats, D.W., Heinbokel, F.J., 1982. A study of reproduction and other life cycle phenomena in planktonic protists using an acridine orange fluorescence technique. Marine Biology 67, 71–79.

Correll, D.L., 1981. Nutrient mass balances for the watershed, headwaters, intertidal zone, and basin of the Rhode River estuary. Limnology and Oceanography 26, 1142–1149.

Correll, D.L., Jordan, T.E., Weller, D.E., 1999. Precipitation effects on sediment and associated nutrient discharges from Rhode River watersheds. Journal of Environmental Quality 28, 1897–1907.

Davies-Colley, R.J., Vant, W.N., Smith, D.G., 1993. Colour and clarity of natural waters. Ellis Horwood.

Dawson, C.E., 1965. Length–weight relationships of some Gulf of Mexico fishes. Transactions of the American Fisheries Society 94, 279–280.

Dickey, T., Frye, D., Jannasch, H., Boyle, E., Manov, D., Sigurdson, D., McNeil, J., Stramska, M., Michaels, A., Nelson, N., Siegel, D., Chang, G., Wu, J., Knap, A., 1998. Initial results from the Bermuda testbed mooring program. Deep-Sea Research I 45, 771–794.

Fenchel, T., Finlay, B.J., 1983. Respiration rates in heterotrophic, free-living protozoa. Microbial Ecology 9, 99–122.

Gallegos, C.L., 2001. Calculating optical water quality targets to restore and protect submersed aquatic vegetation: overcoming

problems in partitioning the diffuse attenuation coefficient for photosynthetically active radiation. Estuaries 24, 381–397.

Gallegos, C.L., 2005. Optical water quality of a blackwater river estuary: the Lower St. Johns River, Florida, USA. Estuarine, Coastal and Shelf Science 63, 57–72.

Gallegos, C.L., Jordan, T.E., 2002. Impact of the Spring 2000 phytoplankton bloom in Chesapeake Bay on optical properties and light penetration in the Rhode River, Maryland. Estuaries 25, 508–518.

Gallegos, C.L., Jordan, T.E., Correll, D.L., 1992. Event-scale response of phytoplankton to watershed inputs in a subestuary: timing, magnitude, and location of phytoplankton blooms. Limnology and Oceanography 37, 813–828.

Gallegos, C.L., Kenworthy, W.J., 1996. Seagrass depth limits in the Indian River Lagoon (Florida, USA): application of an optical water quality model. Estuarine, Coastal and Shelf Science 42, 267–288.

Gallegos, C.L., Neale, P.J., 2002. Partitioning spectral absorption in case 2 waters: discrimination of dissolved and particulate components. Applied Optics 41, 4220–4233.

Gallegos, C.L., Correll, D.L., Pierce, J.W., 1990. Modeling spectral diffuse attenuation, absorption, and scattering coefficients in a turbid estuary. Limnology and Oceanography 35, 1486–1502.

Gallegos, C.L., Jordan, T.E., Correll, D.E., 1997. Interannual variability in spring bloom timing and magnitude in the Rhode River, Maryland (USA): observations and modeling. Marine Ecology Progress Series 154, 27–40.

Harding, L.W.J., Magnuson, A., Mallonee, M.E., 2005. SeaWiFS retrievals of chlorophyll in Chesapeake Bay and the mid-Atlantic bight. Estuarine, Coastal and Shelf Science 62, 75–94.

Hines, A.H., Haddon, A.M., Wiechert, L.A., 1990. Guild structure and foraging impact of blue crabs and epibenthic fish in a subestuary of Chesapeake Bay. Marine Ecology Progress Series 67, 105–126.

Hu, C., Muller-Karger, F.E., Biggs, D.C., Carder, K.L., Nababan, B., Nadeau, D., Vanderbloemen, J., 2003. Comparison of ship and satellite bio-optical measurements on the continental margin of the NE Gulf of Mexico. International Journal of Remote Sensing 24, 2597–2612.

Jones, S.E., Jago, C.F., Bale, A.J., Chapman, D., Howland, R.J.M., Jackson, J., 1998. Aggregation and resuspension of suspended particulate matter at a seasonally stratified site in the southern North Sea: physical and biological controls. Continental Shelf Research 18, 1283–1309.

Jordan, T.E., Pierce, J.W., Correll, D.L., 1986. Flux of particulate matter in the tidal marshes and subtidal shallows of the Rhode River estuary. Estuaries 9, 310–319.

Jordan, T.E., Correll, D.L., Miklas, J., Weller, D.E., 1991. Nutrients and chlorophyll at the interface of a watershed and an estuary. Limnology and Oceanography 36, 251–267.

Kirk, J.T.O., 1992. Monte Carlo modeling of the performance of a reflective tube absorption meter. Applied Optics 31, 6463–6468.

Kirk, J.T.O., 1994. Light and Photosynthesis in Aquatic Ecosystems, second ed. Cambridge University Press.

Leipe, T., Loeffler, A., Emeis, K.-C., Jaehmlich, S., Bahlo, R., Ziervogel, K., 2000. Vertical patterns of suspended matter characteristics along a coastal-basin transect in the western Baltic Sea. Estuarine, Coastal and Shelf Science 51, 789–804.

van Leussen, W., 1988. Aggregation of particles, settling velocity of mud flocs, a review. In: Dronkers, J., van Leussen, W. (Eds.), Physical Processes in Estuaries. Springer-Verlag, pp. 347–403.

Maa, J.P.-Y., Lee, C.-H., 1997. Variation of the resuspension coefficients in the lower Chesapeake Bay. Journal of Coastal Research 25, 63–74.

Maa, J.P.-Y., Sanford, L.P., Halka, J.P., 1998. Sediment resuspension characteristics in Baltimore Harbor, Maryland. Marine Geology 146, 137–145.

Malone, T.C., Conley, D.J., Fisher, T.R., Glibert, P.M., Harding, L.W., Sellner, K.G., 1996. Scales of nutrient-limited phytoplankton productivity in Chesapeake Bay. Estuaries 19, 371–385.

McPherson, B.F., Miller, R.L., 1987. The vertical attenuation of light in Charlotte Harbor, a shallow, subtropical estuary, south-western Florida. Estuarine, Coastal and Shelf Science 25, 721–737.

Mobley, C.D., 1994. Light and water. Radiative transfer in natural waters. Academic Press, New York.

Montagnes, D.J.S., Lynn, D.H., 1993. A quantitative protargol stain (QPS) for ciliates and other protists. In: Kemp, P.F., Sherr, B.F., Sherr, E.B., Cole, J.J. (Eds.), Handbook of Methods in Aquatic Microbial Ecology. Lewis Publishers, pp. 229–240.

Olmi III, E.J., Bishop, J.M., 1983. Variations in total width–weight relationships of blue crabs, *Callinectes sapidus*, in relation to sex, maturity, molt stage and carapace form. Journal of Crustacean Biology 3, 575–581.

Pempkowiak, J., Beldowski, J., Pazdro, K., Staniszewski, A., Leipe, T., Emeis, K.-C., 2002. The contribution of the fine sediment fraction to the fluffy layer suspended matter (FLSM). Oceanologia 44, 513–527.

Postma, H., 1967. Sediment transport and sedimentation in the estuarine environment. In: Lauff, G.H. (Ed.), Estuaries. American Association for the Advancement of Science, Washington, DC, pp. 158–179.

Rabalais, N.N., Turner, R.E., 2001. Coastal hypoxia: consequences for living resources and ecosystems. American Geophysical Union.

Richardson, K., Jørgensen, B.B., 1996. Eutrophication: definition, history and effects. In: Jørgensen, B.B., Richardson, K.R. (Eds.), Eutrophication in Coastal Marine Ecosystems. American Geophysical Union, pp. 1–19.

Sanford, L.P., 1994. Wave-forced resuspension of upper Chesapeake Bay muds. Estuaries 17, 148–165.

Scheffer, M., Portielje, R., Zambrano, L., 2003. Fish facilitate wave resuspension of sediment. Limnology and Oceanography 48, 1920–1926.

Shimeta, J., Amos, C.L., Beaulieu, S.E., Ashiru, O.M., 2002. Sequential resuspension of protists by accelerating tidal flow: implications for community structure in the benthic boundary layer. Limnology and Oceanography 47, 1152–1164.

Southwick, C.H., Pine, F.W., 1975. Abundance of submerged vascular vegetation in the Rhode River from 1966 to 1973. Chesapeake Science 16, 147–151.

Stramski, D., Mobley, C.D., 1997. Effects of microbial particles on oceanic optics: a database of single-particle optical properties. Limnology and Oceanography 42, 538–549.

Stross, R.G., Sokol, R.C., 1989. Runoff and flocculation modify underwater light environment of the Hudson River estuary. Estuarine, Coastal and Shelf Science 29, 305–316.

Stumpf, R.P., Pennock, J.R., 1989. Calibration of a general optical equation for remote sensing of suspended sediments in a moderately turbid estuary. Journal of Geophysical Research 94, 14,363–14,371.

Stumpf, R.P., Pennock, J.R., 1991. Remote estimation of the diffuse attenuation coefficient in a moderately turbid estuary. Remote Sensing of Environment 38, 183–191.

Twardowski, M.S., Donaghay, P., 2001. Separating in situ terrigenous sources of absorption by dissolved materials in coastal waters. Journal of Geophysical Research 106, 2545–2560.

Zaneveld, J.R.V., Kitchen, J.C., Moore, C., 1994. The scattering error correction of reflecting-tube absorption meters. In: Ackleson, S. (Ed.), Ocean Optics XII. SPIE, pp. 44–55.